Chloride Effect on the Early Photolysis Intermediates of a Gecko Cone-Type Visual Pigment†

James W. Lewis,‡ Jie Liang,§ Thomas G. Ebrey,§ Mordechai Sheves,|| and David S. Kliger*,‡

Department of Chemistry and Biochemistry, University of California, Santa Cruz, California 95064, Biophysics Program and Department of Cell and Structural Biology, University of Illinois at Urbana-Champaign, Urbana, Illinois 61801, and Department of Organic Chemistry, Weizmann Institute of Science, Rehovot 76 100, Israel

Received June 27, 1994; Revised Manuscript Received December 5, 1994⊗

ABSTRACT: Nanosecond laser photolysis measurements were conducted on the cone-type visual pigment P521 in digitonin extracts of Tokay gecko (*Gekko gekko*) retina containing physiological chloride ion levels and also on samples which had been chloride depleted or which contained high levels (4 M) of chloride. Absorbance difference spectra were recorded at a sequence of time delays from 30 ns to 60 μs following excitation with a pulse of either 532- or 477-nm actinic light. Global analysis showed the kinetic decay data for gecko pigment P521 to be best fit by two exponential processes under all chloride conditions. The initial photoproduct detected had a broad spectrum characteristic of an equilibrated mixture of a Batho P521 intermediate with its blue-shifted intermediate (BSI P521) decay product. The first exponential process was assigned to the decay of this mixture to the Lumi P521 intermediate. The second exponential process was identified as the decay of Lumi P521 to Meta I P521. The initial photoproduct's spectrum exhibited a strong dependence on chloride concentration, indicating that chloride affects the composition of the equilibrated mixture of Batho P521 and BSI P521. These results suggest that the affinity for chloride is reduced ~5-fold in the Batho P521 intermediate and ~50-fold in the BSI P521 intermediate. Chloride concentration also affects the apparent decay rate of the equilibrated mixture. When the apparent decay rate is corrected for the composition of the equilibrated mixture, a relatively invariant microscopic rate constant is obtained for BSI decay ($k = 1/55$ ns^{-1}). The rate constant obtained agrees with the value observed for the synthetic 9-*cis*-α-retinal gecko pigment which has a completely forward-shifted equilibrium mixture, indicating that the BSI decay is controlled by a relaxation process independent of chromophore and chloride concentration and thus presumably characteristic of the gecko opsin protein.

Two types of receptor cells can typically be found in vertebrate retinas. Rod cells provide visual information under conditions of dim illumination, while cone cells provide the higher level visual information obtainable in brighter light. Whereas a good deal has been learned regarding the processes which occur after light is absorbed by rhodopsin, the visual pigment of most rod cells, little is known about the intermediate species which appear after photolysis of the cone cell visual pigments. A number of factors favor study of rod cells. These include the reduced stability of cone pigments relative to rhodopsin and the vast abundance of rhodopsin compared to cone pigments in most easily available (e.g., bovine) retinas. Another significant factor is that there are usually several different cone pigments with distinct absorption spectra present in the retina, and it is difficult to prepare individual cone pigments for photochemical study.

The lack of experimental data on the photochemistry of cone pigments is unfortunate because their functionally important variability constitutes a perturbation which could be useful in unraveling the mechanism of vision. In addition to variability with amino acid sequence, human red and green cone pigment absorbances are affected by the presence of chloride ion. This constitutes another variable which could potentially be manipulated to elucidate mechanism. A further unique aspect of cone pigments is the interesting behavior reported for the chicken red cone pigment, iodopsin, where a thermal back-reaction of the first photointermediate occurs at low temperatures (Yoshizawa & Wald, 1967). It has been proposed that bound chloride inhibits a chromophore relaxation required for bleaching of the pigment (Imamoto *et al.*, 1989). This unusual barrier to the forward progress of visual transduction can only be studied in a cone pigment since no analogous barrier has been found in rhodopsin.

It has long been known that the major pigment of the Tokay gecko (*Gekko gekko*) retina, P521, displays a chloride effect similar to iodopsin (Crescitelli, 1977). The significance of this was not completely clear initially since P521 occurs in rod-like cells and constitutes an unusually large fraction of the pigment in the gecko retina. However, P521 is a cone-type pigment since its amino acid sequence is very similar to that of the chicken and human long-wavelength cone pigments (Kojima *et al.*, 1992). Moreover, gecko P521 possesses the same amino acid motif which has recently been shown to form the chloride binding site in the human red and green cone pigments (Wang *et al.*, 1993). It thus seems that gecko retina can provide relatively pure samples for photochemical studies of cone visual pigment transduction.

† This research was supported by the National Institutes of Health (Grants EY00983 to D.S.K. and EY01323 to T.G.E.).

* Author to whom correspondence should be addressed.
‡ University of California, Santa Cruz.
§ University of Illinois, Urbana-Champaign.
|| Weizmann Institute of Science.

⊗ Abstract published in *Advance ACS Abstracts,* April 15, 1995.

0006-2960/95/0434-5817$09.00/0

The gecko retina provides only about one-eighth the pigment of a bovine retina. Until recently this precluded study of the early intermediates at physiological temperatures since an impracticably large number of animals would be required to produce the amounts of pigment needed for photochemical characterization with a traditional time-resolved spectral apparatus. We have overcome these limitations by developing an apparatus which can obtain a sequence of time-resolved difference spectra from a submilligram amount of visual pigment (Lewis & Kliger, 1993). Here we report observations of the early intermediates which appear on the 30-ns to 60-μs time scale after photolysis of this gecko cone-type pigment and their dependence on chloride concentration.

EXPERIMENTAL PROCEDURES

Sample Preparation. Frozen retinas containing ~1.2 OD units of gecko pigment in pH 7.4 MOPS buffer, 100 mM KCl, 5 mM $MgCl_2$, and 1 mM DTT were prepared from eight gecko eyes as previously described (Liang *et al.*, 1993). Immediately prior to photochemical characterization the retinas were thawed, depleted of chloride if necessary [two washes with distilled water (Sorvall SS-34 rotor, 17K rpm, 30 min) followed by resuspension in pH 7.0 TRIS buffer with 100 mM K_2SO_4], spun down (Sorvall SS-34, 12K rpm, 20 min), and then homogenized thoroughly with a glass pipet at 4 °C in 1.2 mL of a 2% digitonin solution containing the salts appropriate for the intended experiment [either *physiological* (pH 7.0, 10 mM TRIS, 60 mM KCl, 40 mM NaCl, 2 mM $MgCl_2$, 0.1 mM EDTA) or *chloride depleted* (pH 7.0, 10 mM TRIS, 100 mM K_2SO_4) or *4 M KCl* (physiological with sufficient KCl added to make 4 M KCl)]. After 90 min, the unsolubilized material was removed by centrifugation (Sorvall SS-34, 5K rpm, 10 min). Typically 70% of the pigment (0.85 OD units with optical purity $\equiv A_{min}/A_{max} \approx 0.54$) was extracted into the supernatant. All operations were carried out in darkness or with very limited use of a Kodak No. 2 safelight.

Kinetic Spectroscopy. Absorbance changes from 400 to 700 nm were measured using an optical multichannel approach described previously (Lewis & Kliger, 1993). Difference spectra were recorded at a series of times from 30 ns to 60 μs after excitation. Single microliter aliquots of pigment suspensions were photolyzed once using laser excitation (150 $\mu J/mm^2$) either at 532 nm from the second harmonic of a Nd:YAG laser or at 477 nm from a dye laser pumped by the third harmonic of the Nd:YAG laser. In either case the ~7-ns duration laser pulse entered the sample perpendicular to the probe light beam and was linearly polarized in the vertical direction. Absorbance changes were measured using a probe light beam which was linearly polarized at 54.7° (magic angle) relative to the actinic light. Limited measurements were carried out using vertically and horizontally polarized probe light to ensure that residual signals at the magic angle due to rotational diffusion were not significant for the conclusions made here (Lewis & Kliger, 1991). In a typical experiment, measurements were repeated at each delay time in groups of four, interspersed with the other delay times, to produce a total of 40 measurements at each delay. All measurements were made at room temperature.

The amplitude of the absorbance changes observed was small (~0.01 absorbance unit) so that even very small distortions which are unimportant for larger signals become significant. Instrumental effects of this type originate from the weak phosphor glow of the optical multichannel analyzer's image intensifier and from pulse to pulse intensity fluctuations of the probe flashlamp. The former distortions were removed by subtracting a baseline measured using an inert sample from all the difference spectra collected. The error introduced by probe variation was dealt with by offsetting the difference spectra at all time delays so that the absorbance change averaged over a wavelength range near 700 nm (where no true absorbance change should take place) was zero. The magnitude of both corrections amounted to less than 0.001 absorbance unit.

Difference absorbance spectra collected at a sequence of times following photolysis were fit globally using previously described methods (Hug *et al.*, 1990). Fits to sums of one, two, and three exponentials were attempted. For a given fit, lifetimes and b-spectra (spectral changes associated with each lifetime) were obtained. Combined with an assumed mechanism, the b-spectra could be used to construct intermediate difference spectra which gave the difference in absorbance between the intermediates which appeared in the assumed mechanism and the "bleach", the pigment changed by photolysis. By adding the bleach spectrum to the intermediate difference spectra, absolute spectra of the intermediate species can be determined. To measure the spectrum of the pigment bleached by the laser pulse, a modification of the previously described procedure was used (Albeck *et al.*, 1989). Instead of using Ammonyx LO to remove absorbance of photoproducts from the wavelength region where the pigment band occurs, 3 mM NH_2OH was added to the special sample used to determine the bleach.

RESULTS

Gecko pigment suspensions in digitonin with physiological chloride levels were intially excited with pulses of 532-nm light. Photolysis at that wavelength produced very small transient changes in optical density from 30 ns to 60 μs following excitation. Even with the poor signal to noise ratio (S/N) it was clear that a red-shifted, bathorhodopsin-like absorber was present immediately after the laser pulse. This first product decayed on the time scale monitored to form products which were spectrally more blue-shifted. By smoothing the data and using only the wavelength region where the signal was largest, global fitting was able to describe the data in terms of a biexponential decay with lifetimes 130 ns and 5.1 μs. Using the lifetimes, the b-spectra, and the bleach spectrum, we constructed absorption spectra for three species appearing sequentially on the time scale of our measurements. In order of appearance these had approximate λ_{max}'s of 550, 520, and 500 nm (data not shown). The most unusual feature of these spectra was the ~130-nm full width at half-maximum (fwhm) of the first species detected. This is much larger than the typical 100-nm fwhm observed for absorption bands of visual pigments and their photolysis intermediates. We suspected that the first species formed was an equilibrated mixture of two photointermediates, but this was uncertain because of the noise level of our initial experiment. Higher S/N was needed to confirm the large spectral breadth of the first intermediate species.

A likely cause of the small amplitude of the time-dependent signals was secondary photolysis of the batho

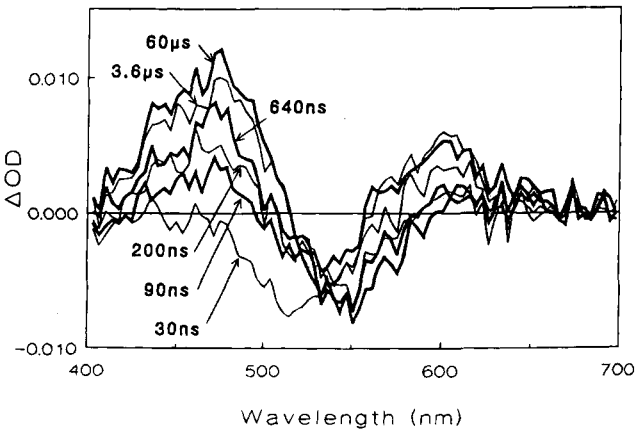

FIGURE 1: Absorbance difference spectra recorded from digitonin extracts of gecko retina containing physiological levels of chloride ion (100 mM). Difference spectra were recorded at delay times from 30 ns to 60 μs after photolysis with a pulse of 477-nm actinic light. Curves are labeled with the delay time at which the spectrum was collected and with line type alternating between light and heavy for successive times. In the red portion of the spectrum the 30-ns trace is the top one, showing transient absorbance in this region which decays away at longer delay times. The data shown in this figure required 0.5 mg of pigment and are representative of several data sets which were collected under these conditions.

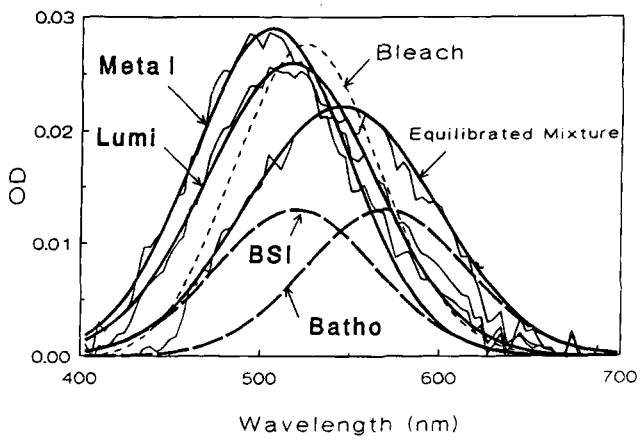

FIGURE 2: Spectra of intermediates observed in digitonin extracts of gecko retina containing physiological levels of chloride ion (100 mM). The data in Figure 1 were best fit by a biexponential process which corresponds to a sequential decay involving three intermediates. The spectra of these intermediates are shown by the light lines in this figure labeled (in order of appearance) equilibrated mixture, Lumi, and Meta I. The spectra of the intermediates were fit to Gaussian functions shown by the heavy lines. The spectrum of the equilibrated mixture was decomposed into the sum of two Gaussian functions shown by the heavy dashed lines labeled Batho and BSI. The lightly dashed line shows the spectrum of the material "bleached" by the laser pulse which was added back to the spectra in Figure 1 to produce these absolute intermediate spectra.

product by the 532-nm excitation pulse. This would be particularly serious for P521 since its iso pigment absorbs relatively far to the blue (Crescitelli, 1982), which could result in an unfavorable photostationary equilibrium mixture for the observation of batho-product decay. To reduce this problem, further experiments were conducted using excitation with pulses of 477-nm light. Typical data obtained from such an experiment are shown in Figure 1. The curves are the difference spectra (absorbance of photoproducts minus absorbance of pigment) collected at varying time delays after photolysis. Significantly higher S/N was obtained using 477-nm excitation than had been achieved using 532 nm. That this increase is indeed due to reduced iso-pigment formation can be seen by the absorbance changes observed near the iso-pigment peak (488 nm) immediately after 477-nm excitation. No positive optical density change is observed in the 30-ns difference spectrum near the iso-pigment peak while at this same point in the spectrum after 532-nm excitation (data not shown) approximately half of the positive absorbance ultimately present at 60 μs was already present at 30 ns. Nearly three times as much batho product was observed to decay thermally after 477-nm excitation as had been observed using 532-nm actinic light.

Above 500 nm the data collected after 477-nm excitation showed the same qualitative features as the data collected after 532-nm excitation. The 30-ns difference spectrum in Figure 1 shows bleaching in the vicinity of the pigment absorption band accompanied by positive absorbance in the red region of the spectrum. This shows that a red-shifted species is detected initially after photolysis. The succeeding difference spectra show this red absorbing material thermally decaying to produce a more blue absorbing species. There does not seem to be a single isosbestic point for all the difference spectra, with the early time value near 550 nm shifting toward 530 nm at later times. The data were of sufficient S/N that they could be fit globally to two exponential processes over the wavelength region shown. No single exponential process was able to fit the data within the noise level of the experiment. Fits using more than two exponentials either diverged or produced fits whose qualitative features were not reproducible. The two-exponential fit was reproducible using 477-nm excitation as well as agreeing reasonably well with the results using 532-nm excitation. The observed lifetimes obtained using 477-nm excitation were 110 ns and 4.8 μs. Assuming the simple sequential model:

$$A \rightarrow B \rightarrow C$$

the results of the two exponential fit were used to construct absolute absorption spectra of the three sequential species (shown in Figure 2). The result of 477-nm excitation confirms the conclusion of the 532-nm experiment; i.e., the spectrum of A is very broad while the spectra of B and C are well within the range normally observed for visual pigments and their photointermediates.

Similar experiments were conducted for gecko pigment samples which had been chloride depleted or which contained 4 M KCl. The results for chloride-depleted gecko pigment are shown in Figure 3. These data were fit to a biexponential model producing lifetimes of 60 and 880 ns. The spectra of the intermediate species deduced from the fit are shown in Figure 4. Substantial differences exist in the spectrum of the first intermediate species compared to that found in the case where physiological chloride levels were present. Photolysis of chloride-depleted gecko pigment produces an initial species which has a narrower bandwidth but whose absorption band is substantially skewed. While the λ_{max} is blue-shifted some 20 nm, there is a pronounced absorbance tail extending to the red. The second and third intermediates produced by chloride-depleted gecko pigment have spectra much more similar to those observed after photolysis of the pigment with physiological levels of chloride present.

Results obtained after photolysis of gecko pigment in the presence of 4 M KCl are shown in Figure 5. Here also the

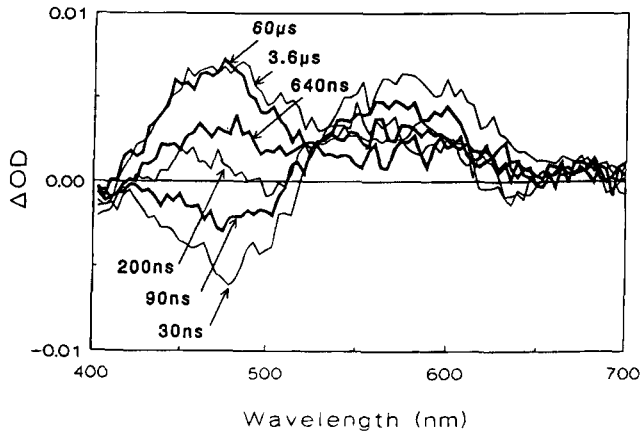

FIGURE 3: Absorbance difference spectra recorded from digitonin extracts of gecko retina which had been depleted of chloride ion. Except for the absence of chloride ion, conditions were the same as in Figure 1.

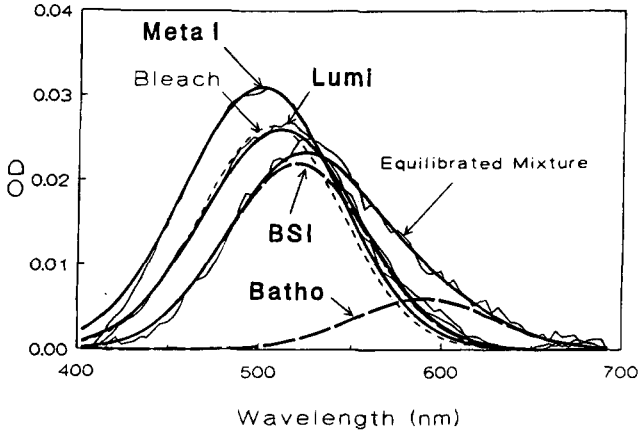

FIGURE 4: Spectra of intermediates observed in digitonin extracts of gecko retina which had been depleted of chloride ion. The spectra of the intermediates were derived from the data in Figure 3 as described in the text and are presented as described in the caption to Figure 2.

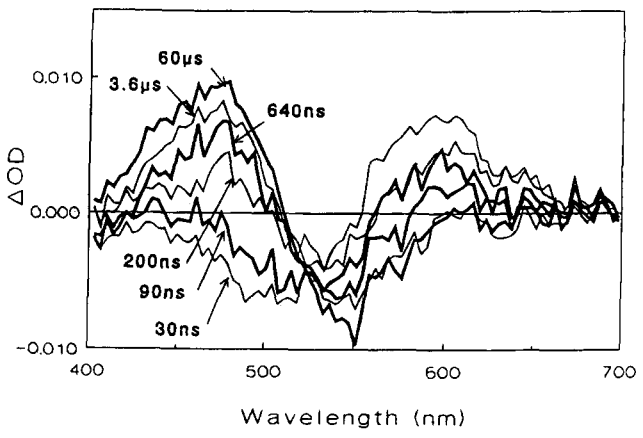

FIGURE 5: Absorbance difference spectra recorded from digitonin extracts of gecko retina containing high levels of chloride ion (4 M). Except for the chloride ion concentration, conditions were the same as in Figure 1.

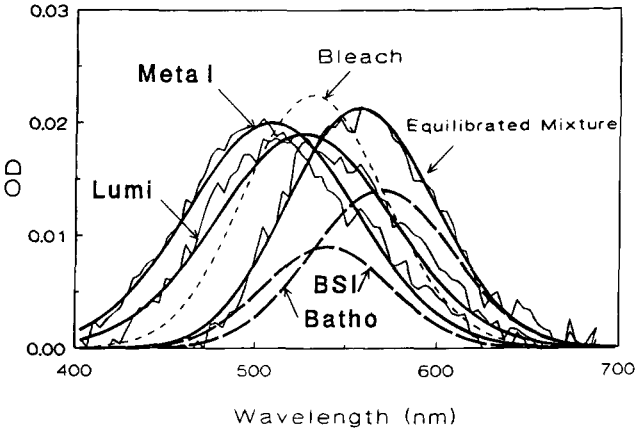

FIGURE 6: Spectra of intermediates observed in digitonin extracts of gecko retina containing high levels of chloride ion (4 M). The intermediate spectra were derived from the data in Figure 5 as described in the text and are presented as described in the caption to Figure 2.

best fit of the data was biexponential with lifetimes of 130 ns and 2.7 μs. Intermediate spectra are shown in Figure 6. Again the largest difference can be seen in the spectrum of the first intermediate species, where there is increased band intensity compared to the spectra of the late intermediates, and there are differences in the shape as well. In 4 M KCl, the first species is red-shifted compared to the first species seen at the lower chloride concentrations, and while no tailing is observed to the red, there is a possible shoulder on the blue edge of the band. The two late intermediates are again similar in characteristics to those observed at lower chloride concentrations, but there may be a red shift of λ_{max}, particularly for B, the second intermediate species.

Digitonin suspensions of rhodopsin were also photolyzed for comparison with gecko pigment results. Typical data are shown in Figure 7. The best fit of these data was biexponential with lifetimes of 60 ± 15 and 480 ± 120 ns. If these data are fit to a straight sequential model as above, the B intermediate has a broad spectrum because rhodopsin photointermediates actually decay via the scheme (Hug *et al.*, 1990):

$$\text{Batho} \overset{K_{eq}}{\rightleftharpoons} \text{BSI} \rightarrow \text{Lumi} \ldots$$

Thus for rhodopsin the short lifetime corresponds to the conversion of a red-shifted Batho intermediate to a blue-shifted intermediate in an approach to the equilibrated mixture of Batho and BSI. The longer lifetime corresponds to the conversion of the equilibrated mixture (with a broad spectrum) to Lumi. Taking into account this actual mechanism, the data in Figure 7 can be converted into absolute absorption spectra of the actual intermediates. In this process some estimate of the K_{eq} is obtained since if too high a value is used the absolute BSI spectrum obtained has unphysical negative values in some regions. The usual K_{eq} value observed for rhodopsin in membranes or octyl glucoside (1.4) gave such negative regions when used for the digitonin data. Thus a lower value (1.0) was used to reconstruct the intermediate spectra shown in Figure 8. The apparent rates observed after photolysis of bovine rhodopsin and gecko pigment are summarized in Table 1.

DISCUSSION

Correspondence of Photoproducts from Gecko P521 and Bovine Rhodopsin. Similarities of function and structure between rhodopsin and the gecko pigment make it likely that there would be many similarities in the mechanism of action as displayed in the sequence of intermediates observed after photolysis. Clear support for this idea comes from the observation described above of a red-shift species after

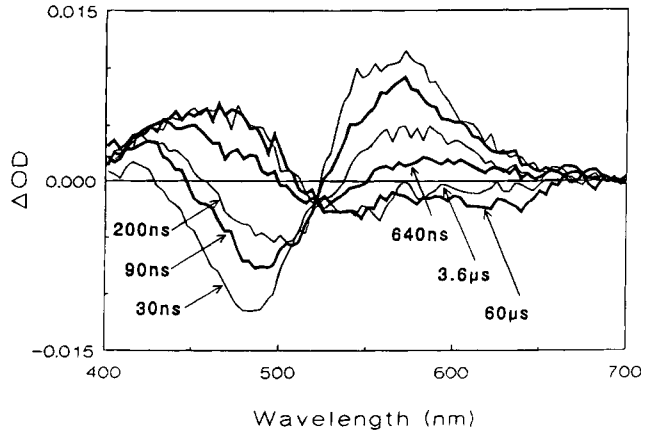

FIGURE 7: Absorbance difference spectra recorded from digitonin extracts of bovine rod outer segments. Conditions were similar to those under which the data in Figure 1 were collected.

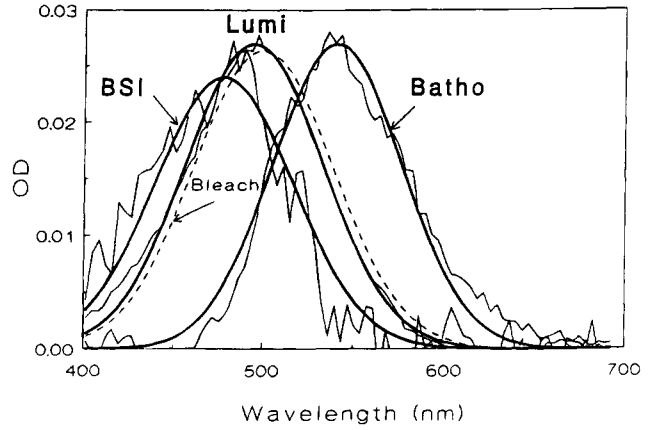

FIGURE 8: Spectra of intermediates observed in digitonin extracts of bovine rod outer segments. The data in Figure 7 were fit globally to two exponential processes. The spectrum of the first intermediate was not abnormally broad (in contrast to the gecko case) and corresponds to the bathorhodopsin (Batho) intermediate. The first decay corresponds to the decay of Batho toward an equilibrated mixture of Batho and the BSI intermediate. The second lifetime describes the decay of the equilibrated Batho−BSI mixture to lumirhodopsin (Lumi). In digitonin, Lumi is stable on the time scale of the measurements shown in Figure 7. Data in this figure are presented using the same conventions as the data in Figure 2.

Table 1: Observed Lifetimes

species	Batho ⇄ BSI	[Batho ⇄ BSI] → Lumi	Lumi → Meta I
bovine rhodopsin (digitonin)	60 ± 15 ns	480 ± 120 ns	
bovine rhodopsin (octyl glucoside)[a]	30 ± 7 ns	220 ± 20 ns	
gecko P-521 (without Cl^-) (digitonin)		60 ns	880 ns
gecko P-521 (physiological Cl^-) (digitonin)		110 ns	4.8 μs
gecko P-521 (4 M KCl) (digitonin)		130 ns	2.7 μs
iodopsin (CHAPS)[b]		130 ns	230 μs

[a] Hug *et al.*, 1990. [b] Shichida *et al.*, 1993.

photolysis in both pigment systems which decays on the nanosecond time scale. However, equally evident from this work are apparent differences in the nature of the species detected after photolysis of the two pigments. In both cases one of the species observed has the character of an equilibrated mixture, but for gecko it is the first species detected while in the rhodopsin case it is the second species observed. The simplest explanation for this difference is that in the gecko case the time resolution of our experiments was insufficient to resolve the decay of the first intermediate, and therefore the first species detected here for gecko is the equilibrated mixture of its batho product and the BSI-like intermediate. Thus, the Batho/BSI mixture seems to equilibrate much more rapidly in the gecko cone-type pigment than in rhodopsin. Support for this interpretation comes from a recent study of the chicken red cone pigment, iodopsin, which assigned the first species observed after photolysis on the nanosecond time scale to the intermediate BL (Shichida *et al.*, 1993) which we believe to be analogous to our equilibrated mixture of Batho and BSI. There also, on a time scale similar to ours, the decay of bathoiodopsin to BL−iodopsin was not resolved. Further similarity between the iodopsin and gecko pigment cases is shown by the 130-ns lifetime observed for the decay of BL−iodopsin to form lumiiodopsin. This is close to the lifetime of the decay of the Batho/BSI mixture to Lumi in gecko and supports the hypothesis that strong parallels exist in the early photochemical behavior of the red-absorbing pigments of these two species. Resonance Raman results for bathoiodopsin conclude that the chromophore is more strained near C14 compared to bathorhodopsin (Lin *et al.*, 1994). Lin *et al.* hypothesize this would destabilize bathoiodopsin relative to bathorhodopsin, consistent with the accelerated cone pigment Batho decay which we propose to explain the broad spectrum of our first detected species.

Although there are two pigments in the gecko retina, P467 and P521, we believe that the intermediates observed in our experiments correspond to those of the P521 pigment of gecko. The amount of P467 present in the gecko retina is an order of magnitude smaller than the amount of P521 (Crescitelli, 1977). Further, batho-product photolysis which so effectively reduces the signal amplitude after 532-nm photolysis of P521 would operate similarly to reduce the contribution of P467 after 477-nm laser excitation. The similarity in the lifetimes observed using 532- and 477-nm excitation also supports the conclusion that P521 is the dominant contributor to the signals we analyze. Finally, the effect of chloride ion concentration on the spectrum of the equilibrated Batho P521 ⇄ BSI P521 mixture (see below) is unlikely to result from P467 since it is a rhodopsin-like pigment and lacks the chloride binding site (Kojima *et al.*, 1992).

Invariance of the Microscopic Rate of BSI Decay. Attribution of the first species we detect to the equilibrated Batho P521 ⇄ BSI P521 mixture implies that the second species detected here is Lumi P521. This conclusion is consistent with the spectrum we detect for the second species which is slightly blue-shifted relative to the spectrum of P521. Similarly, the final intermediate detected here, with a spectrum slightly more intense and blue-shifted relative to Lumi P521, would then be Meta I P521. Overall, except for acceleration of some rates, our data suggest that P521 excitation results in the same basic sequence of intermediates which prevail in rhodopsin, namely:

Batho P521 ⇄ BSI P521 → Lumi P521 → Meta I P521 ...

More significant differences occur in the later intermediates, and these have been recently described (Liang *et al.*, 1993).

Table 2: λ_{max}'s of Intermediates: Wavelength/fwhm (nm)

species	Batho	BSI	Lumi	Meta I
bovine rhodopsin (digitonin)	542/83	481/88	496/90	
gecko P-521 (without Cl^-)	590[a]/92	520/92	511/100	500/100
gecko P-521 (physiological Cl^-)	570/107	520/107	516/110	506/103
gecko P-521 (4 M KCl)	570/92	540/83	527/115	509/112
α-iso gecko P-521		430/67	463/88	455/92

[a] This value is uncertain due to the small amplitude of this component.

Table 3: Maximum Absorbance of Intermediates

species	Batho	BSI	Lumi	Meta I	K_{eq}
bovine rhodopsin (digitonin)	0.027	0.021	0.027		1.0
gecko P-521 (without Cl^-)	0.006	0.022	0.026	0.031	4
gecko P-521 (physiological Cl^-)	0.012	0.012	0.024	0.026	1
gecko P-521 (4 M KCl)	0.014	0.009	0.019	0.029	0.6
α-iso gecko P-521		0.005	0.007	0.008	>10

Table 4: Microscopic Rate Constant for BSI P-521 Decay

pigment	BSI decay rate constant (ns^{-1})
gecko P-521 (without Cl^-)	1/50
gecko P-521 (physiological Cl^-)	1/55
gecko P-521 (4 M KCl)	1/50
α-iso gecko P-521	1/60

Study of artificial rhodopsin pigments produced from retinal analogs has shown that while chromophore character can dramatically affect the Batho ⇄ BSI equilibrium constant, for many chromophores the microscopic rate constant for BSI decay has the value ~1/110 ns (Randall *et al.*, 1991). Even though this microscopic rate constant is invariant, the *apparent* rates of decay in the artificial pigments can vary greatly downward from this value because for many pigments only a fraction of the decaying equilibrated mixture is in the BSI form. Here, in the case of P521, the varying spectrum of the first species detected shows that another factor, the chloride concentration, affects the equilibrium constant as well. It is of interest to determine what the microscopic rate constant for BSI decay is for the gecko protein and further whether it is independent of chloride concentration.

Estimation of the microscopic rate constant for BSI decay requires determination of the amounts of Batho P521 and BSI P521 present in the equilibrated mixture. Under the present circumstances this can only be estimated crudely. Figures 2, 4, and 6 show decomposition of the first species detected in terms of two components with Gaussian profiles. Tables 2 and 3 give the relevant parameters for these. Assuming that the extinction coefficients of Batho P521 and BSI P521 are comparable (as they are for rhodopsin in digitonin), equilibrium constants which prevail at the three chloride concentrations can be estimated. These are given in Table 3. Microscopic BSI P521 decay rate constants were determined by multiplying the apparent rate (the reciprocal of the first observed lifetime) by the reciprocal of the fraction of BSI present in the equilibrium mixture. While the K_{eq} varies from 4 to 0.6, the microscopic rate constant for BSI P521 decay remains invariant at ~1/55 ns within the experimental uncertainty of our measurements (Table 4). This indicates that the protein relaxation triggered by BSI formation is a factor of 2 faster for P521 than it is for bovine rhodopsin. Support for this conclusion comes from observation of a 1/60-ns initial decay rate for the iso-α-retinal artificial pigment of P521 (data not shown) where, as in the bovine artificial pigment case, the equilibrium is completely forward shifted, making the microscopic rate equal to the apparent rate.

Scheme 1

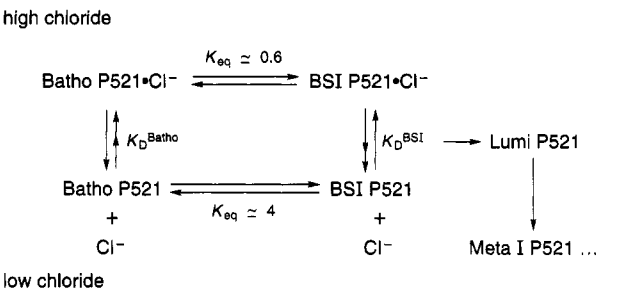

Chloride Dissociation Constants of the Intermediates. The observed chloride effect on the Batho P521 ⇄ BSI P521 equilibrium constant is unexpected on the basis of the ~2 mM Cl^- binding constant which can be estimated from titration of the chloride effect on the P521 spectrum (Crescitelli, 1982). For our kinetic measurements the bulk of the effect on K_{eq} takes place in the vicinity of 100 mM chloride ion. Clearly, at least one of the later intermediates binds chloride less tightly than does P521 itself. While the observations have something of the character of a simple binding where Batho P521 binds chloride while BSI P521 does not, the binding curve required by such a mechanism is too steep a function of concentration to agree with our measurements. A more consistent model is shown in Scheme 1. The binding constants for chloride are determined as follows: From the experiment at low chloride (summarized in Table 3) we know [BSI P521] = 4[Batho P521] and from the high chloride experiment [BSI P521•Cl^-] = 0.6[Batho P521•Cl^-]. These can be substituted into the equilibrium constant expression for the physiological (100 mM) chloride case to obtain an expression for the ratio of [Batho P521]/[Batho P521•Cl^-]. Since this value occurs for [Cl^-] = 100 mM, the binding constant for Batho P521 can be determined. The BSI P521 chloride binding constant can be determined similarly. This model fits our data if the chloride binding constants are chosen to be $K_D^{BSI} \simeq 90$ mM and $K_D^{Batho} \simeq 10$ mM. Scheme 1 shows that after photolysis there is a reduction in the affinity for chloride at Batho P521 and a further major reduction at BSI P521. Since these changes occur at such an early stage in the bleaching sequence, it is likely that only the chromophore or its immediate pocket environment is involved.

The chloride binding site is known to be composed of two positive charges, His 196 and Lys 199 (corresponding to positions 181 and 184 in bovine rhodopsin) (Wang *et al.*, 1993; Kojima *et al.*, 1992). In rhodopsin Glu 181 provides negative charge where the Cl^- binding site in P521 has a net positive charge. It is tempting to speculate about how charge differences in this region of these two proteins affect the spectra of their photolysis intermediates. However, such speculation is probably premature at this time.

The λ_{max}'s of Batho P521 and BSI P521 given in Table 2 depend on chloride concentration. That feature of our model is not essential to the more fundamental conclusion that a major reduction in chloride binding occurs at the BSI P521 stage. A similar conclusion would result from the assump-

tion that Batho P521 and BSI P521 have chloride-independent spectra. *A priori*, there is no reason to prefer the latter, more restrictive model since Lumi P521 and Meta I P521 both show a systematic red shift induced by chloride. This behavior is more certain than the Batho P521 and BSI P521 cases since the Lumi P521 and Meta I P521 λ_{max}'s are determined from discrete species detected directly and not from decomposition of the spectrum of an equilibrated mixture. Thus, given that P521 and two of its intermediates have chloride-dependent spectra, it is possible that its Batho and BSI spectra have some dependence on chloride concentration as well. Our results do not show a discernible trend in the λ_{max} of Batho P521 (the only variation, for chloride-depleted P521, is probably uncertain due to the small size of the Batho component under those conditions). BSI, on the other hand, does show a possible chloride effect with the value in 4 M KCl being 20 nm to the red of the chloride-depleted case. With the present experimental resolution it is unclear whether Cl^- affects the Batho P521 and BSI P521 λ_{max}'s, but when higher time resolution measurements, capable of resolving the approach to equilibrium, become feasible, it should be possible to determine whether Batho P521 and BSI P521 have chloride-dependent spectra.

The chloride effect on the Batho P521 $\rightleftharpoons$ BSI equilibrium may have relevance for the thermal reversion of bathoiodopsin observed at low temperature in the presence but not in the absence of chloride (Imamoto *et al.*, 1989). Since BSI formation is required for bleaching, the barrier to release of chloride in frozen samples could restrict the pigment to a BSI formation mechanism less favorable to thermal bleaching. Given that BSI formation in rhodopsin is entropically driven (Hug *et al.*, 1990), at low temperatures the barrier to BSI formation may be greater than the thermal barrier to back-isomerization, therefore allowing thermal reversion.

Decay of Lumi P521 is much faster than the analogous process in rhodopsin. While there is a large uncertainty in the Lumi P521 slow lifetime due to the sparse late time measurements, it seems likely that the chloride-depleted Lumi P521 decays faster than Lumi P521 at either of the other chloride concentrations studied here. This could signify that at the lumi stage the protein returns to a chloride binding constant which approximates that of P521 itself and that the unbound form decays more rapidly to Meta I P521 compared to the chloride bound form of Lumi P521. The rebinding of chloride at the lumi stage is not the only model which could account for post-BSI changes in rates, however, since it is also possible that some structural changes have time constants sufficiently long that Lumi P521 from chloride-depleted P521 remains structurally different from Lumi P521 formed from P521 which has released chloride only at the BSI stage.

Order of magnitude differences also exist between the 4.8-μs Lumi P521 lifetime in digitonin and the 230-μs lifetime reported for lumiiodopsin in CHAPS PC (Shichida *et al.*, 1993). These again may be due to specific differences between gecko and chicken pigments. Another possible cause of differences at this later stage in the bleaching sequence is the difference in detergents used in these two studies.

Study of P521 provides insight into the role of chloride in regulating the early bleaching sequence of cone pigments. An unexpected result has been the observed change in the interaction of the chromophore with the chloride binding site at the BSI stage. As a consequence, an improved structural picture can be drawn, not just of the BSI of cone pigments but also of rhodopsin itself. Such a structural picture is important in understanding the nature of the protein change initiated by BSI formation, an event which has potential significance beyond the visual pigments in the much larger family of heptahelical membrane receptor proteins.

REFERENCES

Albeck, A., Friedman, N., Ottolenghi, M., Sheves, M., Einterz, C. M., Hug, S. J., Lewis, J. W., & Kliger, D. S. (1989) *Biophys. J. 55*, 233−241.

Crescitelli, F. (1977) in *Handbook of Sensory Physiology* (Crescitelli, F., Ed.) Vol. VII/5, pp 391−449, Springer-Verlag, Heidelberg.

Crescitelli, F. (1982) in *Methods in Enzymology* (Packer, L., Ed.) Vol. 81, Academic Press, New York, NY.

Hug, S. J., Lewis, J. W., Einterz, C. M., Thorgeirsson, T. E., & Kliger, D. S. (1990) *Biochemistry 29*, 1475−1485.

Imamoto, Y., Kandori, H., Okano, T., Fukada, Y., Shichida, Y., & Yoshizawa, T. (1989) *Biochemistry 28*, 9412−9416.

Kojima, D., Okano, T., Fukada, Y., Shichida, Y., Yoshizawa, T., & Ebrey, T. (1992) *Proc. Natl. Acad. Sci U.S.A. 89*, 6841−6845.

Lewis, J. W., & Kliger, D. S. (1991) *Photochem. Photobiol. 54*, 963−968.

Lewis, J. W., & Kliger, D. S. (1993) *Rev. Sci. Instrum. 64*, 2828−2833.

Liang, J., Govindjee, R., & Ebrey, T. G. (1993) *Biochemistry 32*, 14187−14193.

Lin, S. W., Imamoto, Y., Fukada, Y., Shichida, Y., Yoshizawa, T., & Mathies, R. A. (1994) *Biochemistry 33*, 2151−2160.

Shichida, Y., Okada, T., Kandori, H., Fukada, Y., & Yoshizawa, T. (1993) *Biochemistry 32*, 10831−10838.

Yoshizawa, T., & Wald, G. (1967) *Nature (London) 214*, 566−571.

Wang, Z., Asenjo, A. B., & Oprian, D. D. (1993) *Biochemistry 32*, 2125−2130.

BI941415Y